The Astrophysical Journal, 647:753–762, 2006 August 20

THE ABUNDANCE OF DISTANT AND EXTREMELY RED GALAXIES: THE ROLE OF AGN FEEDBACK IN HIERARCHICAL MODELS

N. Menci, A. Fontana, E. Giallongo, A. Grazian, and S. Salimbeni
INAF—Osservatorio Astronomico di Roma, Via di Frascati 33, 00040 Monteporzio, Italy
Received 2006 February 6; accepted 2006 April 28

ABSTRACT

We investigate the effect of AGN feedback associated with the bright QSO phase on the color distribution of galaxies from $z = 0$ up to $z = 4$. To this aim, we insert a blast-wave model of AGN feedback in our semianalytic model of galaxy formation, which includes the growth of supermassive black holes and the AGN activity triggered by interactions of the host galaxies. The AGN feedback is directly related to the impulsive, luminous quasar phase. We test our model by checking the consistency of its results against (1) the QSO luminosity functions from $z = 0$ to 4, and (2) the observed local relation between the black hole mass $m_{\rm BH}$ and the mass of the host galaxy. At low redshift the inclusion of AGN feedback enhances the number of red bright galaxies so that the color distribution of $M_r < -22$ objects is entirely dominated by red ($u - r > 1.5$) galaxies; at $0.5 < z < 2$ it yields a rest-frame $U - V$ color distribution, in agreement with existing observations. In the range $z \approx 1.5$–2.5, we find that 31% of galaxies contribute to the extremely red object (ERO) population with $m_K < 20$ (Vega system); at such a magnitude, the model yields an ERO surface density of 6.3×10^3 deg^2, matching existing data. Extending our analysis to $z = 4$, the model matches the observed surface density 1.5×10^3 deg^2 of distant red galaxies (DRGs) at $m_K = 20$; such a population is predicted to be dominated by galaxies with old stellar populations for $z > 2.5$.

Subject headings: cosmology: theory — galaxies: active — galaxies: formation — galaxies: high-redshift

Online material: color figures

1. INTRODUCTION

The color distribution of galaxies constitutes a key observable to constrain models of galaxy formation in a cosmological context. In fact, the most delicate sector of such models is that linking the age of stellar populations (closely related to the color) to the depth of the growing dark matter (DM) potential wells (hence the luminosity) of the galaxies hosting them. Indeed, while hierarchical models predict massive objects to be assembled at later cosmic times, they also predict their progenitor clumps to be formed in biased high-density regions of the primordial density field, where the enhanced density allowed early star formation.

Thus, the abundance of red, massive galaxies predicted by such models results from the balance between the later epoch of assembly predicted for the most massive objects and the older stellar population predicted to be in place in the progenitors of such objects. Such a delicate balance makes the comparison with the observations concerning the abundance and the color distribution of massive galaxies a sensible probe for such models.

Indeed, recent models, including the enhancement in the star formation of progenitors of massive galaxies triggered by interactions, are able to match many global properties of the evolving galaxy population, such as the observed decline of the global stellar mass density from $z = 0$ to 2 (see, e.g., Fontana et al. 2004) and the evolution of the B and UV luminosity functions (Somerville et al. 2001; Menci et al. 2004; Dahlen et al. 2005) from $z = 0$ to 4. The bimodal feature of the observed local color distribution (Strateva et al. 2001; Baldry et al. 2004; Bell et al. 2004; Giallongo et al. 2005) is also obtained in recent versions of hierarchical models (Kang et al. 2005; Menci et al. 2005; Bower et al. 2006; Croton et al. 2006), so the existence of two well-defined populations appears to stem from the interplay between the biasing properties of the primordial density field—originating the DM condensations constituting the progenitors of galaxies—and the star formation and feedback processes driving the evolution of baryons in such progenitors.

Despite the above successes in matching the global behavior of galaxy evolution, when one focuses on the observed proportion of red/blue galaxies, it is found that current hierarchical models underestimate the number of luminous/massive *red* galaxies. The models (Menci et al. 2005; Croton et al. 2006, with no active galactic nucleus [AGN] feedback) addressing the bimodal color distribution of local galaxies are characterized by an excess of massive ($M_r < -22$) galaxies in the blue ($u - r < 1.5$) branch of the local color distribution compared to the red one; a similar deficit of luminous red galaxies is present in other semianalytic models of galaxy formation (Somerville et al. 2004). At higher redshift the problem is even more severe: the abundance of EROs (with optical infrared colors redder than a passively evolving elliptical, $R - K > 5$) at $z \approx 1$–2.5 is underestimated by present hierarchical models (see McCarthy 2004; Cimatti et al. 2004; Daddi et al. 2005; Somerville et al. 2004) by factors up to 10 (depending on the exact color and magnitude cut). This suggests that an additional process must be at work in determining the observed properties of galaxies; the overall agreement of hierarchical model predictions with the global (not color-selected) evolutionary properties of galaxies discussed above suggests that such a process should not constitute the main driver but rather a complementary physical mechanism affecting mainly the evolution of the bright galaxy population.

In this respect, a possible solution has been proposed in terms of the feedback from AGNs hosted at the center of galaxies (see, e.g., Ciotti & Ostriker 1997; Silk & Rees 1998; Haehnelt et al. 1998; Fabian 1999). Indeed, the role of the energy injection from the AGNs into the interstellar medium of the host galaxies is at present one of the most pressing issues in the study of galaxy evolution, both on the observational and on the theoretical side.

On the one hand, blueshifted absorption lines in the UV and X-ray spectra of active galaxies reveal the presence of massive

outflows of ionized gas from their nuclei; they are characterized by high velocities (up to $0.4c$) indicating mass flows of 1–10 $M_\odot$ yr^{-1} (see Crenshaw et al. 2003; Chartas et al. 2002, 2004; Pounds et al. 2003). Further evidence based on the radio and X-ray observations of galaxies (Böringer et al. 1993; Fabian et al. 2000; McNamara et al. 2000) indicates that bubbles of radio-emitting plasma are present in elliptical galaxies containing supermassive black holes (SMBHs). On larger scales, fast (1000 km s^{-1}) massive (10–50 $M_\odot$ yr^{-1}) flows of neutral gas are observed through 21 cm absorption of radio-loud AGNs (see Morganti et al. 2005), indicating that AGNs have a major effect on the circumnuclear gas in the central kiloparsec region of AGNs. Since the powers of outflows are similar to (or even exceed) the observed bolometric luminosities and the cooling losses, these observations indicate that the feedback from AGNs has to be considered among the processes that regulate the evolution of baryons in the galactic potential wells and, of course, the growth of the SMBHs in the host galaxy.

On the theoretical side, the impact of AGN feedback on galaxy formation has been investigated in a number of papers (Murray et al. 2005; Monaco & Fontanot 2005; Begelman & Nath 2005; Scannapieco & Oh 2004; Scannapieco et al. 2005); all the different assumed mechanisms for the energy injection can produce the expulsion of a significant fraction of the interstellar gas; the effectiveness of the AGN feedback in quenching the BH growth and the subsequent star formation has been confirmed by recent aimed simulations of galaxy collisions triggering AGN activity (Di Matteo et al. 2005) and of AGN feeding activated by gas infall (Kawata & Gibson 2005). However, inserting such a mechanism into a cosmological framework of galaxy formation constitutes a challenging task. The model by Granato et al. (2004) successfully uses the shining of quasi-stellar objects (QSOs) as a clock for the formation of elliptical galaxies, but does not include spiral galaxies or provide predictions for the lower energy AGNs at $z < 1$. In ab initio hierarchical models of galaxy formation in a cosmological context (Bower et al. 2006; Cattaneo et al. 2006; Croton et al. 2006; Kang et al. 2006), SMBHs are assumed to grow during galaxy mergers both by merging with other BHs and through gas accretion, the latter being described in terms of tunable scaling laws. The inclusion of AGN feedback in these models allows suppression of the cooling in massive halos (a long-standing problem of hierarchical models); however, such feedback must be still at work at low redshift to continuously suppress star formation in massive halos at $z \lesssim 1$. Since the QSO activity drops sharply for $z \lesssim 2.5$, these authors assume the energy feedback responsible for the suppression of the cooling to be effective only in halos that undergo quasi-static cooling; the feedback is associated with a continual and quiescent accretion of hot gas onto the SMBHs. In these models the feedback mechanism is thus associated only with a smooth accretion process, which is not the main driver of BH growth, so they do not focus on the evolution of the luminous properties of QSOs and of the bright AGN sources.

Here we aim to investigate the effect of the feedback directly associated with the observable QSOs and luminous AGNs on galaxy formation. To this aim we include the AGN feedback model developed by Lapi et al. (2005) in our semianalytic model of galaxy formation (Menci et al. 2004, 2005), which includes the growth of SMBHs through gas accretion triggered by galaxy encounters. The AGN feedback we include in the present paper is substantially different from the implementations in Croton et al. (2006), Bower et al. (2005), and Cattaneo et al. (2006), since it is produced during the short AGN active phase, sweeping the cold gas content of the galaxies in a way similar to that found in the simulations by Di Matteo et al. (2005); in addition, since it is associated with the observable active phase of AGNs, the feedback effect we investigate is mainly produced at high redshift. Before exploring the impact of such an impulsive form of AGN feedback on galaxy formation, we first test against observations the predicted evolution of the luminosity functions of QSOs from $z = 4$ to the present, since the feedback we consider is directly related to their emission. After checking the consistency with the observed local $m_{\rm BH}$-σ relation between the BH mass $m_{\rm BH}$ and the one-dimensional velocity dispersion σ of the host galactic bulges, we compute the galaxy color distribution at low ($z \lesssim 0.1$) and high (up to $z = 3$) redshifts, discussing the effect of the AGN feedback on such distributions. Since the distinctive feature of our AGN feedback model (associating the feedback with the bright QSO phase) is an effect peaking at redshift $1.5 < z < 3.5$, we focus particularly on the properties of high-redshift galaxies, and we compare these with the observed number density of EROs up to $z = 2.5$ and of DRGs selected by the observed frame $J - K > 2.3$ (Franx et al. 2003; van Dokkum et al. 2003), up to $z \approx 4$. In § 4 we discuss our results.

2. THE MODEL

We adopt the semianalytic model (SAM) of galaxy formation described in Menci et al. (2005); this connects the baryonic processes (gas cooling, star formation, and supernovae feedback) to the merging histories of the DM halos (with mass M, virial radius R, and circular velocity V) and of the galactic subhalos (with mass m, radius r, and circular velocity v) following the canonical recipes adopted by SAMs of galaxy formation (Kauffman et al. 1993; Cole et al. 2000; Somerville & Primack 1999; Somerville et al. 2001; Menci et al. 2002, 2004; Okamoto & Nagashima 2003).

The host DM halos contain hot gas (with mass m_h) at the virial temperature T. The fraction of such a gas, which is able to radiatively cool, settles into a rotationally supported disk with gas mass m_c; the disk radius r_d and rotation velocity v_d are computed after the model by Mo et al. (1998). The merging histories of the host halos, and the dynamical friction and binary aggregations acting on the included subhalos, are computed adopting the canonical Monte Carlo technique as in Menci et al. (2005). We keep the implementation of gas cooling, star formation, and feedback described in the above paper, with the same choice of free parameters (the normalization of the star formation timescale and of the feedback efficiency).

The integrated stellar emission from galaxies is computed convolving the star formation rate resulting from our model with the synthetic spectral energy distributions from Bruzual & Charlot (1993), adopting a Salpeter initial mass function (IMF). The dust extinction affecting the intrinsic galactic luminosities is computed assuming the dust optical depth to be proportional to the metallicity of the cold phase (computed assuming a constant effective yield) and to the disk surface density (see Menci et al. [2002] for further details). When not otherwise specified, we assume a Galaxy extinction curve. We have shown in our previous paper that the model is able to produce a Tully-Fisher relation, cold gas and disk size distributions, and B-band galaxy luminosity functions (from $z = 0$ to $z \approx 4$), in good agreement with observations. As for the growth of SMBHs with the associated AGN emission, and for the corresponding AGN feedback, we adopt the models by Cavaliere & Vittorini (2000) and Lapi et al. (2005), respectively. Here we recall their basic points.

2.1. *The Growth of SMBHs*

The growth of SMBHs is implemented as described in Menci et al. (2003); the accretion of cold gas is triggered by galaxy

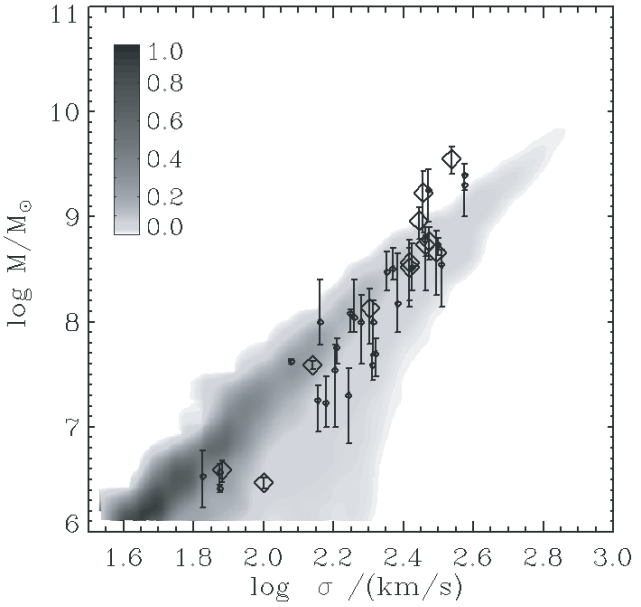

FIG. 1.—Relation between the BH mass $M_{\rm BH}$ and the one-dimensional velocity dispersion σ of the bulges of the host model galaxies at $z = 0$, compared with data from Ferrarese & Merritt (2000; *diamonds*) and Gebhardt et al. (2000; *circles*). [*See the electronic edition of the Journal for a color version of this figure*.]

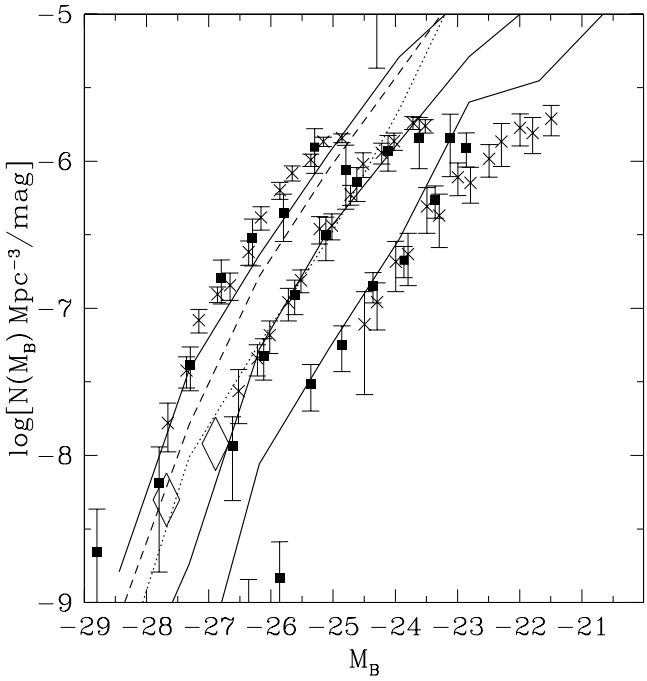

FIG. 2.—QSO *B*-band luminosity functions from our model (*solid lines*), shown for $z = 0.55$ (*lower curve*), $z = 1.2$ (*middle curve*), and $z = 2.2$ (*upper curve*), compared with the data points. These are taken from Hartwick & Shade (1990; *squares*) and Boyle et al. (2000; *crosses*), and rescaled to our cosmology with $\Omega_0 = 0.3$, $\Omega_\lambda = 0.7$, and $h = 0.7$. We also show the model results for $z = 3$ (*dashed line*) and $z = 4$ (*dotted line*), compared to the SDSS data at $z = 4.2$ from Fan et al. (2001; *diamonds*). The blue luminosity L_B has been obtained by applying a bolometric correction of 13 (Elvis et al. 1994) to the bolometric luminosity in eq. (3). [*See the electronic edition of the Journal for a color version of this figure*.]

encounters (both flyby and merging), which destabilize part of the available cold gas. The rate of interactions is (Menci et al. 2003)

$$\tau_r^{-1} = n_T \Sigma(r_t,\, v,\, V_{\rm rel}) V_{\rm rel}. \quad (1)$$

Here n_T is the number density of galaxies in the same halo, and $V_{\rm rel}$ is their relative velocity. The encounters effective for angular momentum transfer require (1) the interaction time to be comparable with the internal oscillation time in the involved galaxies (resonance), and (2) the orbital specific energy of the partners not to exceed the sum of their specific internal gravitational energies. The cross section Σ for such encounters is given by Saslaw (1985) in terms of the distance $r_t \approx 2r$ for a galaxy with given v (see Menci et al. 2003).

The fraction of cold gas accreted by the BH in each interaction event is computed in terms of the variation Δj of the specific angular momentum $j \approx Gm/v_d$ of the gas, to read (Menci et al. 2003)

$$f_{\rm acc} \approx \frac{1}{8}\left|\frac{\Delta j}{j}\right| = \frac{1}{8}\left\langle \frac{m'}{m}\,\frac{r_d}{b}\,\frac{v_d}{V_{\rm rel}}\right\rangle. \quad (2)$$

Here b is the impact parameter, evaluated as the average distance of the galaxies in the halo. Also, m' is the mass of the partner galaxy in the interaction, and the average runs over the probability of finding such a galaxy in the same halo where the galaxy m is located.

The average cold gas accreted during an accretion episode is thus $\Delta m_{\rm acc} = f_{\rm acc} m_c$, and the duration of an accretion episode, i.e., the timescale for the QSO to shine, is assumed to be the crossing time for the destabilized cold gas component, $\tau = r_d/v_d$.

The bolometric luminosity thus produced by the QSO hosted in a given galaxy is then given by

$$L(v,\, t) = \frac{\eta c^2 \Delta m_{\rm acc}}{\tau}. \quad (3)$$

We adopt an energy-conversion efficiency $\eta = 0.1$ (see, e.g., Yu & Tremaine 2002). The SMBH mass $m_{\rm BH}$ grows through the accretion described above and by coalescence with other SMBHs during galaxy merging. As an initial condition, we assume small seed BHs of mass $10^2\ M_\odot$ (Madau & Rees 2001) to be initially present in all galaxy progenitors; our results are insensitive to the specific value as long as it is smaller than $10^5\ M_\odot$.

In our Monte Carlo model, at each time step, we assign to each galaxy the probability of interaction, after the rate given in equation (1). According to such a probability, we assign an active BH accretion phase (with duration τ) to the considered galaxy and compute the accreted cold gas and associated QSO emission through equations (2) and (3).

2.2. *The Feedback from AGNs*

To explore the dynamical effect of feedback occurring during the active AGN phase on the interstellar medium, we adopt the model by Lapi et al. (2005). They compute the effect of an energy injection ΔE by AGNs on the surrounding gas by solving, in the "shell approximation," the equations for a blast wave propagating outward in the interstellar gas, including the effects of gravity and of the gas density gradient. The perturbed gas is confined to a shell with outer (shock) radius $R_s(t)$, which sweeps the gas around the AGN; the effect is similar to that found in the simulations by Di Matteo et al. (2005), although the latter have been performed only in selected cases of major mergers, while our treatment applies also to less energetic events (the accretion rate and hence the energy ΔE injected by the AGN are determined by eq. [2]).

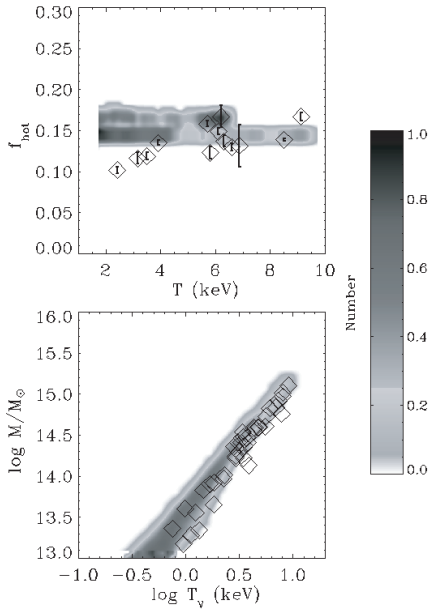

FIG. 3.—*Top:* The relation between the baryon fraction and the X-ray temperature T of the hot gas in groups and clusters of galaxies resulting from the model is compared with observational data points from Lin et al. (2003); the color code refers to the logarithm of the abundance of groups/clusters normalized to its maximum value. *Bottom:* The predicted relation between the mass M of groups and clusters of galaxies and the X-ray temperature of the hot gas; the observational data points are taken from Figuenov et al. (2001). Color code as above. [*See the electronic edition of the Journal for a color version of this figure.*]

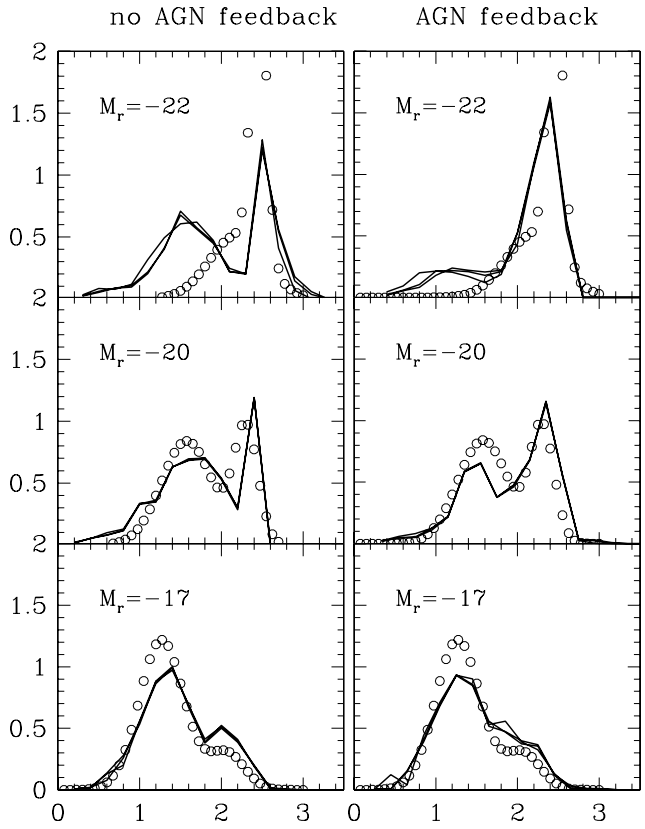

FIG. 4.—Predicted rest-frame $u - r$ color distributions (*heavy lines*) for different dust extinction laws, compared with the Gaussian fit to the SDSS data (from Baldry et al. 2004; *open circles*) for different magnitude bins. The left column refers to the model without the inclusion of AGN feedback, while the right column shows the results when AGN feedback is turned on. The distributions are normalized to the total number of galaxies in the magnitude bin. [*See the electronic edition of the Journal for a color version of this figure.*]

The mass Δm expelled out of the virial radius by the blowout is computed as a function of the ratio $\Delta E/E$, where E is the gas binding energy. The values of Δm and β for any given ratio $\Delta E/E$ are tabulated in Cavaliere et al. (2002), the former being well approximated (to better than 10%) by $\Delta m/m \approx 0.5\Delta E/E$ for $\Delta E/E < 1.4$.

In our semianalytic model, for any galaxy undergoing an active AGN phase (see § 2.1), we compute $\Delta E = fL\tau$ assuming the AGN feedback efficiency $10^{-2} \lesssim f \lesssim 10^{-1}$ as a free parameter, the lower value being more appropriate to radio-quiet AGNs because of the flat spectrum and the low photon momenta; observations of wind speeds up to $v_w \approx 0.4c$ suggest values around $v_w/2c \approx 10^{-1}$, associated with covering factors of order 10^{-1} (see Chartas et al. 2002; Pounds et al. 2003). We then compute the fraction Δm of cold gas expelled by AGNs; the galactic cold gas expelled by the AGN feedback enriches the hot gas phase, which fills the DM potential wells of the structure (group or cluster) hosting the galaxy. Expanding out of the galaxy, the blast wave also expels a tiny fraction of the hot gas in the host structure and resets the hydrostatic equilibrium of such a hot gas to a new temperature, $T + \Delta T$, larger than the initial temperature T by a factor $1/\beta$ (with values in the range 1–1.1 in most cases), also computed after Cavaliere et al. (2002).

3. RESULTS

Here we present our results for a ΛCDM cosmology with $\Omega_0 = 0.3$, $\Omega_\lambda = 0.7$, a baryon fraction $\Omega_b = 0.05$, and Hubble constant $h = 0.7$ in units of 100 km s^{-1} Mpc^{-1}. The star formation and stellar feedback parameters are the same as in Menci et al. (2005), while the AGN feedback efficiency (see § 2.2) is set to $f = 0.05$.

3.1. *Testing the Model: The AGN Evolution and the Intergalactic Gas*

Since our feedback is tightly related to the active AGN phase, we require the model to match not only the observables concerning the galaxy population, but also those concerning the AGN population, in order to have a reliable modelization for the interplay between the cooling and star formation processes and the growth of the SMBH with the ensuing AGN emission and feedback.

Thus, we first show in Figure 1 the $m_{\rm BH}$-σ relation to check that, when integrated over time, the BH accretion that we implement in our model is consistent with the local observations for the whole range of galactic mass spanned by the model. Note that the spread in the $m_{\rm BH}$-σ increases for decreasing galactic mass, a feature shared by all hierarchical models and related to the increasing number of merging histories involved in the formation of massive halos, which results in a lower statistical deviation. Note also that our average relation remains close to a power law, at variance, e.g., with the Bower et al. (2006) model, which predicts a steepening of the relation for large σ; in fact, such a steepening is due to the second "mode" of BH growth implemented in that model, associated with the smooth accretion of hot gas and which ensures that the luminosity of the BH is sufficient to quench cooling in the most massive halos.

Since the time behavior of the energy injection from AGNs is crucial in determining the effects on the galaxy properties, and in our model such injection is related to the active QSO phase,

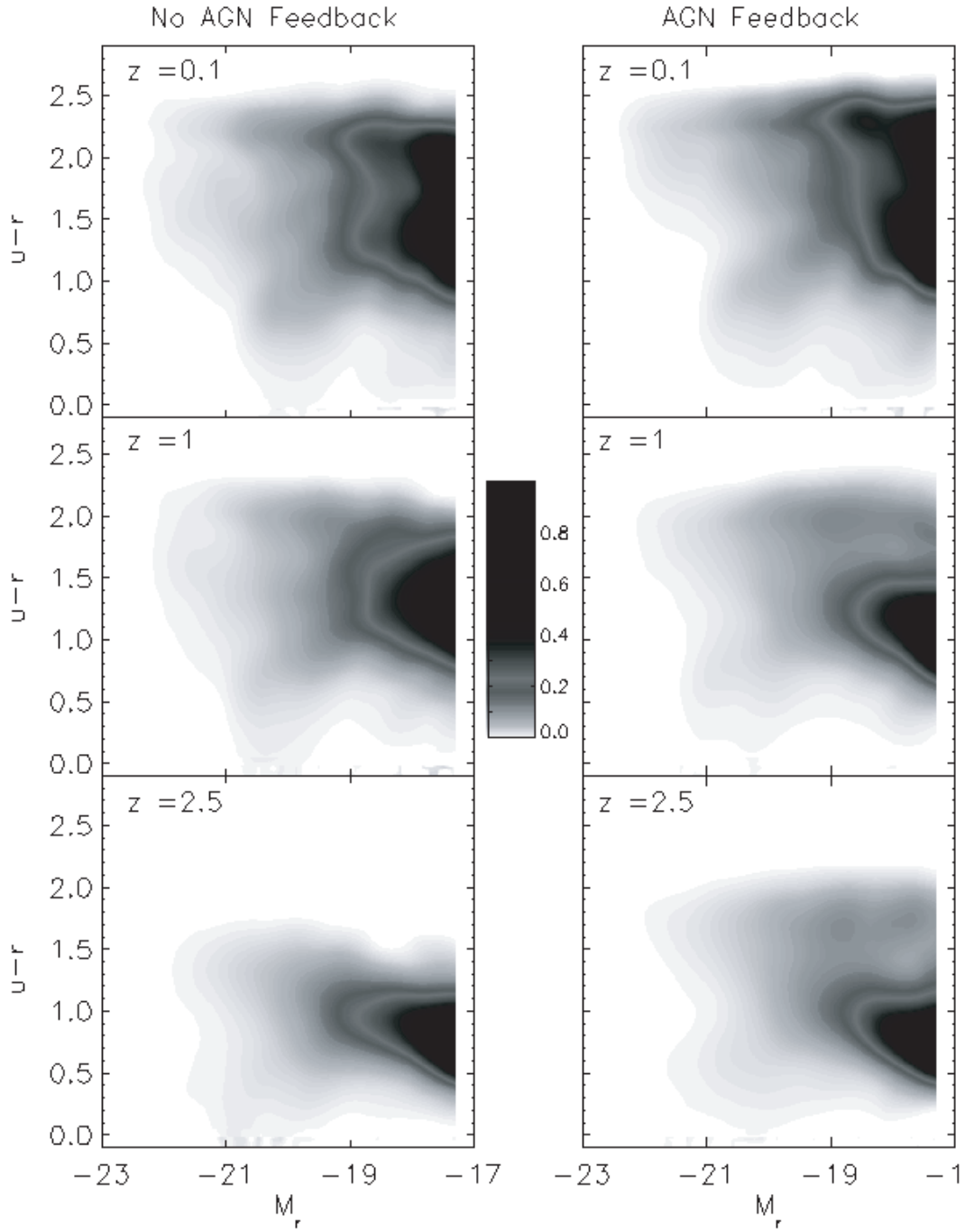

FIG. 5.—The $(u - r)$-M_r relations for the model with no AGN feedback (*left column*) and for the model including the AGN feedback (*right column*) at different redshifts. The color code refers to the number density of galaxies in a given color-magnitude bin, normalized to the maximum value attained at the considered redshift. [*See the electronic edition of the Journal for a color version of this figure.*]

we test in Figure 2 the evolution of the QSO luminosity distribution by comparing it with the observations from $z = 0$ up to 4. Note that our model is able to match the observed decline in the population of bright sources from $z = 2$ to the present; this is due to (1) the decline of merging events refueling the cold gas reservoir of the galaxies; (2) the exhaustion of such a reservoir, due to its earlier conversion in stars; (3) the decline in the rate of interactions (triggering the active accretion phase); and (4) the decrease of the effectiveness of interactions in destabilizing the cold gas (see eq. [1] and the discussion in Menci et al. 2003).

As a final test, we also probe the model predictions for the hot gas phase that is enriched by the gas expelled from the galaxies by the AGN feedback (see § 2.2). In particular, we show in Figure 3 how the baryon fraction and the mass-temperature relation resulting from the model compares with present observations. This shows that (1) the amount of hot gas (enriched by the blow-out of cold galactic gas due to the AGN feedback) is not enhanced over the baryon fraction in groups and clusters and (2) the temperature of the hot gas is not enhanced by the contribution from AGNs up to values exceeding the observations for a given cluster

mass. Indeed, the value of β (§ 2.2) stays close to unity for typical values of the energy ΔE injected by AGNs. The agreement with observations is not unexpected; indeed, while the AGNs are expected to produce significant effects on the cold gas contained in the shallow potential wells of galaxies (and hence to appreciably affect the star formation history of galaxies, which entirely depends on the cold gas phase), the relative variation in the hot gas mass (which is an order of magnitude larger than the m_c) remains, however, small, and has little effect on the baryon fraction in groups and clusters of galaxies. In fact, for such structures the ratio $\Delta E/E$ (see § 2.2) is much less than unity due to their deep potential wells (large gas binding energy E), at least for our assumed value of the AGN feedback efficiency $f \approx 10^{-2}$, so relative changes in the temperature ($\Delta T/T \lesssim 0.1$) and hot gas mass ($\Delta m/m_h \lesssim 0.05$) remain much smaller than 1.

3.2. *The Bimodal Color Distribution of Galaxies*

The effect of the energy injection from AGNs on the color distribution of local galaxies is shown in Figure 4 for three luminosity bins and is compared with the data from the Sloan Digital Sky Survey (SDSS) given in Baldry et al. (2004) for the $u - r$ colors; details on the SDSS u and r bands are given by the above authors. As expected, the AGN feedback affects only the color distribution of luminous galaxies; this is due to their larger cross section for interactions (triggering the AGN activity) and to the larger fraction of destabilized gas accreted by the SMBH (powering the AGN activity). Note also that both the *bimodal partition* and the *downsizing* (i.e., the correlation between the age of the stellar population, or the color, and the galaxy luminosity) are not determined by the AGN feedback, as we showed in our previous paper and as confirmed by the recent results by Croton et al. (2006). Rather, the AGN feedback affects the partition of galaxies between the blue and the red population, enhancing the fraction of red galaxies. In particular, the distribution of very luminous ($M_r < -22$) galaxies is dominated by red objects when AGN feedback is included, in agreement with observations.

At higher redshift, we expect the effect of the AGN feedback directly related to the bright QSO phase to be even more important, due to the enhanced AGN activity at such cosmic epochs. This is first shown in Figure 5, where we show the color-magnitude relation at various redshifts for the model with no AGN energy injection and the model where the AGN feedback is included.

Note that the energy injection from AGNs affects appreciably the number of red galaxies at redshifts $z \gtrsim 2$. In particular, at such redshifts, bimodality only appears in the model including the AGN feedback, while at lower redshifts, $z = 1$–2, the bimodal partition of the color distribution is appreciably enhanced by the effect of AGNs.

To perform a more quantitative comparison between the predicted and the observed bimodal properties of the galaxy population at intermediate and high redshifts, in Figures 6 and 7 we compare these properties with the observational results from the Great Observatories Origins Deep Survey (GOODS) database. We show in Figure 6 the B-band luminosity functions of the red and blue components at different redshifts and compare them with the GOODS data (S. Salimbeni et al. 2006, in preparation). According to the selection criterion discussed in Giallongo et al. (2005), in this plot we define the blue and the red population as those separated by the rest-frame color $U - V = \alpha(19.9 + M_B) + (U - V)_0$ (Vega system), where the parameters α and $(U - V)_0$ are given in the caption for the three redshift bins. At high redshifts ($z \gtrsim 2$) the model with no AGN feedback substantially underestimates the number of red objects, while the

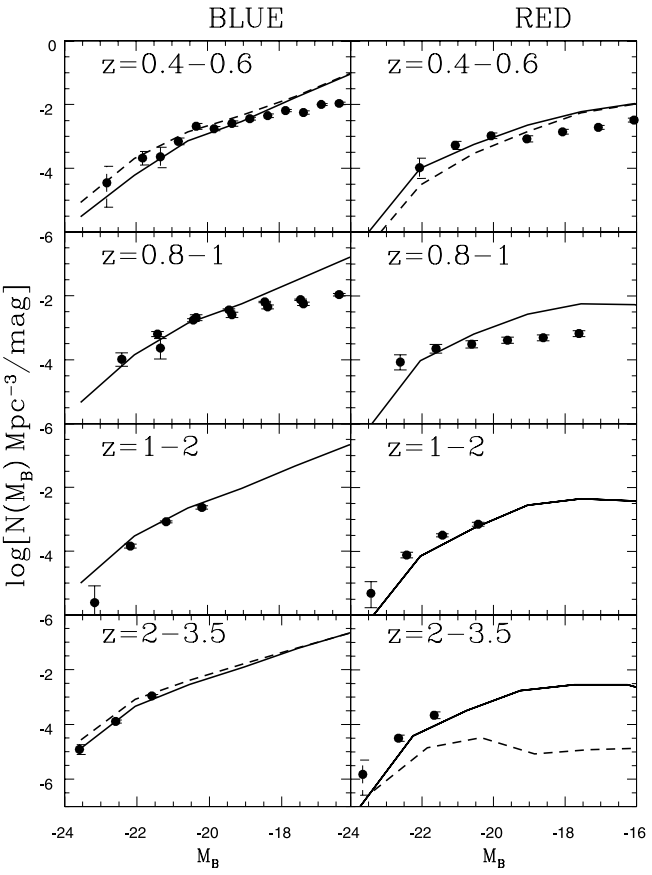

FIG. 6.—Predicted B-band luminosity functions for the blue (*left column*) and the red (*right column*) population at different z (*solid lines*), compared with the GOODS data (S. Salimbeni et al. 2006, in preparation). The dashed lines show the model results when no AGN feedback is included. The parameters for the color separation between the two populations (see text) are $\alpha = -0.084$, -0.081, -0.083, and -0.083 for the 0.4–0.6, 0.8–1, 1–2, and 2–3 redshift bins, respectively; the corresponding values of $(U - V)_0$ are 0.66, 0.58, 0.53, and 0.43. The Vega system is adopted for magnitudes. [*See the electronic edition of the Journal for a color version of this figure.*]

model including the AGN energy injection produces a reasonable agreement at all redshifts for both the blue and the red population, although the long-standing problem of the overprediction of faint objects is still present in the model.

Note also how the galaxies effectively reddened by the inclusion of the AGN feedback constitute a minor fraction of the galaxies contributing to the B- and UV-band luminosity; although the abundance of bright galaxies in the UV and B bands is indeed decreased by the inclusion of the AGN feedback (see top left and bottom left panels of Fig. 6), the resulting luminosity functions are still consistent with the data.

A direct comparison of the predicted and the observed color distribution of galaxies at intermediate redshifts $z = 1$–2 is performed in Figure 7 for three magnitude bins, to show how the model matches the observed early (at $z \approx 2$) appearance of the same downsizing effect that marks the color distribution at low redshifts (see Fig. 4 legend), indicating that the model captures the observed *early* decline of the star formation rate in massive, bright galaxies.

3.3. *The Color Distribution and Abundance of EROs*

From the discussions above, and from inspection of Figure 5, we expect that the inclusion of the AGN feedback will solve the

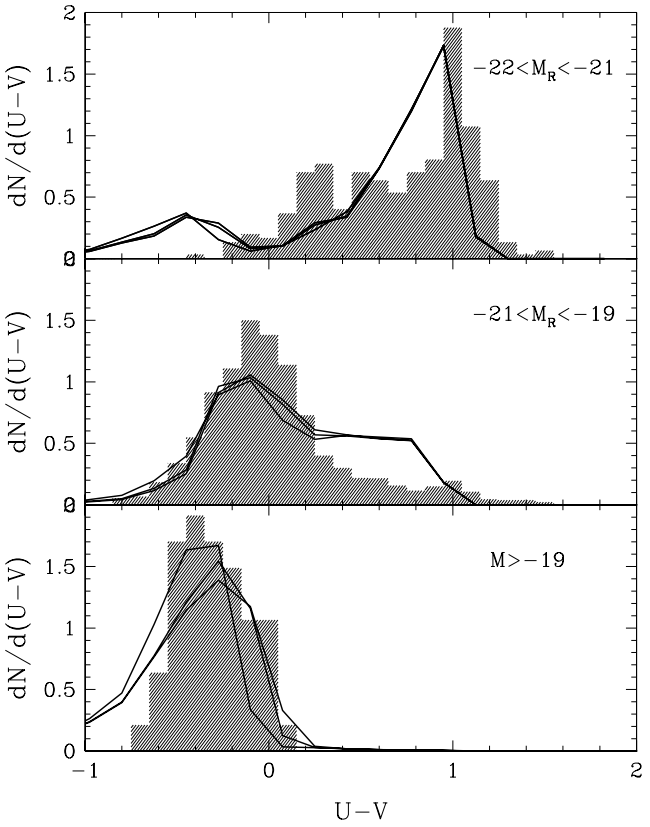

FIG. 7.—Rest-frame $U - V$ color distribution of galaxies in the redshift range $1 < z < 2$ for the R-band magnitude bins $M_r > -19$, $-21 \leq M_r \leq -19$, and $-22 \leq M_r < -21$. The model predictions are the solid lines (for Galaxy, SMC, or Calzetti extinction curves), while the histograms represent the GOODS data from S. Salimbeni et al. (2006, in preparation). [*See the electronic edition of the Journal for a color version of this figure.*]

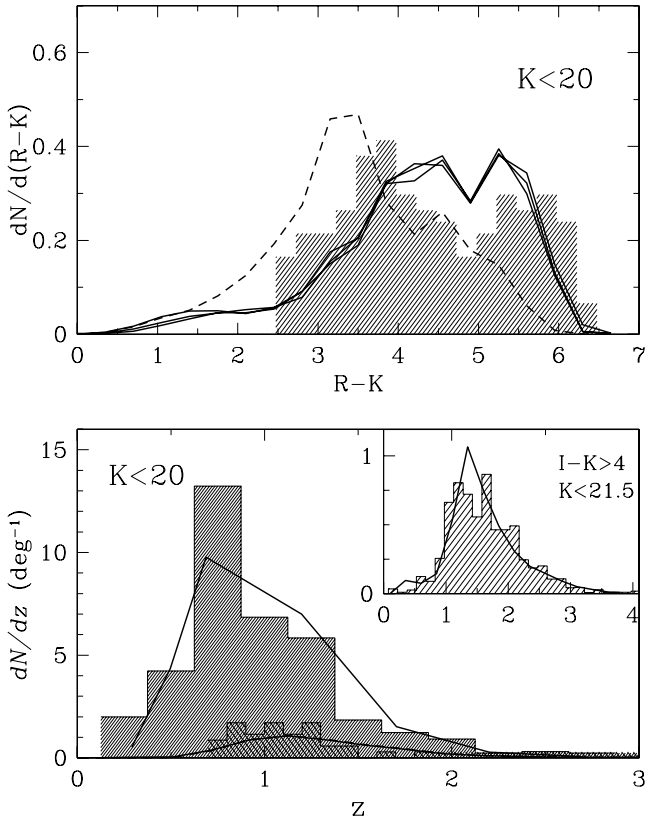

FIG. 8.—*Top:* The observed-frame $R - K$ color distribution from the GOODS data (*histogram*; taken from Somerville et al. 2004) is compared with the results of the model with no AGN feedback (*dashed line*) and of the model including the AGN feedback (*solid line*). *Bottom:* The redshift distribution of $K < 20$ (Vega system) galaxies in the GOODS survey (*histogram*; taken from Somerville et al. 2004) is compared with the results of our model (*solid line*). The lower histogram (taken from Cimatti et al. 2002) and curve represent the observed and the model redshift distribution of the ERO population (normalized to the total number of objects for graphical reasons), respectively. The inset shows the redshift distribution of galaxies selected by $I - K > 4$ down to $m_K = 21.5$; we compare with GOODS data from the catalog described in Grazian et al. (2006; *histogram*). [*See the electronic edition of the Journal for a color version of this figure.*]

long-standing problem of semianalytic models related to their severe underestimate of EROs (with observed $R - K > 5$) at $z \approx 1.5$–2.5 (see McCarthy 2004; Cimatti et al. 2004; Daddi et al. 2005; Somerville et al. 2004) that we recall in § 1. Such a point is addressed in Figure 8, where we plot the observed-frame $R - K$ color distribution of $K < 20$ (Vega system) galaxies in the redshift range $1.7 < z < 2.5$ and compare it with the observed distribution. Note how the inclusion of AGN feedback strongly enhances the number of predicted EROs (see also Fig. 5, *bottom right*), yielding a fraction, 0.31, of objects with $R - K > 5$, close to the observed value, 0.35. The normalization of both data and model predictions is provided by the redshift distribution of $K < 20$ galaxies shown in the bottom panel of Fig. 8. The same panel also shows how the model matches the observed z-distribution of $m_K < 20$ EROs and (in the inset) the distribution of $I - K > 4$ galaxies down to $m_K = 21.5$ to probe the predictions of the model for the most luminous galaxies up to redshift $z = 3$.

Note that the matching between the model *global* (not color-selected) redshift distributions and the observations is not due to the effect of AGN feedback. Indeed, this is due to the effect of starbursts triggered not only by mergers (such as, e.g., in the model by Somerville et al. 2004) but also by galaxy flyby events (see Menci et al. 2003); the latter produce starbursts with a lower efficiency, $\approx$0.1–0.4 (at $z \gtrsim 3$) for a single event, but dominate the encounter statistics due to the high rate of flyby events at such redshifts; the point is discussed in detail in Menci et al. (2003).

The predictions in Figure 8 constitute a distinctive feature of our model, in which the AGN feedback is associated with the bright AGN (QSO) phase (at variance with the other existing semianalytic model, in which it is associated with a smooth accretion phase, continuing down to low redshift), thus strongly acting on the properties of galaxies at $1.5 \lesssim z < 3.5$, when the AGN activity reaches its maximum. Thus, we expect that in our model the density of EROs at magnitudes fainter than $m_K = 20$ (contributed by high-redshift objects) to be still rising. Such a specific prediction of our model is shown in Figure 9, where we plot the differential magnitude counts of EROs resulting from our model. The model is able to match the observed value, $\approx 6.3 \times 10^3$ deg^{-2}, for the surface density of EROs with magnitude $m_K \approx 20$, and predicts a continuous increase in the ERO surface density to reach values $\approx 3 \times 10^4$ deg^{-2} at $m_K = 22$.

Note that agreement of the model with observations holds not only for all EROs, but also in detail for density of dust-free passive EROs, which constitute about 80% of all EROs in our model. This is shown in the bottom panel of Figure 9, where we compare the model predictions for the cumulative number counts of EROs without dust extinction with the data concerning passive dust-free EROs presented by Miyazaki et al. (2003).

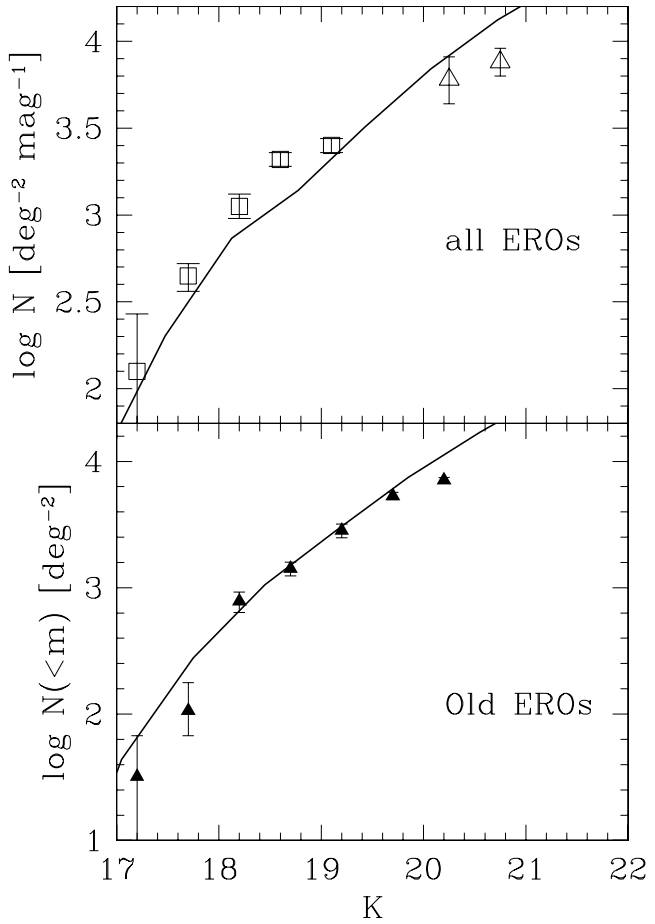

FIG. 9.—*Top:* The surface density of EROs (per unit magnitude) as a function of their *K*-band magnitude resulting from the model is compared with data from Roche et al. (2003; *triangles*) and Daddi et al. (2000; *squares*). *Bottom:* The *cumulative* surface density of EROs *without dust extinction* (*solid line*) is compared with data concerning the dust-free passive EROs taken from Miyazaki et al. (2003). [*See the electronic edition of the Journal for a color version of this figure.*]

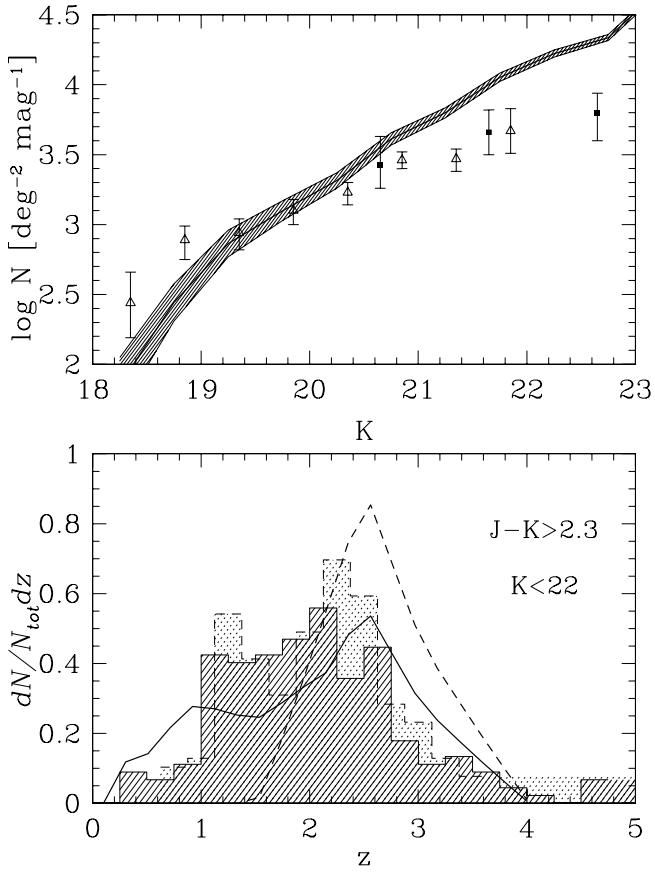

FIG. 10.—*Top:* The predicted surface density (per unit magnitude) of DRGs is plotted as a function of their *K*-band magnitude (*solid line*). The hatching shows the uncertainty due to the different adopted extinction curves. We compare with data from Grazian et al. (2006). *Bottom:* The predicted redshift distribution of DRGs with $m_K < 20$ (*solid line*) is compared with the GOODS data from Grazian et al. (2006; *solid histogram*); we also show the Hubble Deep Field (HDF)/*Spitzer* observations by Papovich et al. (2006; *dashed histogram*) for galaxies selected by stellar mass $m_* > 10^{11}\ M_\odot$. The model prediction in absence of dust extinction is shown as a dashed line. Both data and observations have been normalized to the total number of objects; their relative normalization is given by the magnitude counts in the top panel. [*See the electronic edition of the Journal for a color version of this figure.*]

3.4. *The Abundance and Redshift Distribution of DRGs*

A more sensible probe for the model predictions at high redshifts is constituted by the observed surface density and redshift distribution of DRGs selected by the criterion $J - K > 2.3$ (Franx et al. 2003; van Dokkum et al. 2003), as shown in Figure 10. The predicted surface density of such objects (*top panel*) matches the observed value 1.5×10^3 deg^{-2} at $m_K = 20$, while at $m_K = 22$ it reaches values $\approx 10^4$ deg^{-2}. Since the $J - K$ color cut allows for selection of red galaxies up to higher redshift compared to EROs, we can probe the model predictions concerning their redshift distribution up to $z \approx 4$ (*bottom panel*); the redshift distribution of the total DRG population is peaked at $z \approx 2.5$, in good agreement with the observed distributions, and shows a minor peak at $z \approx 1$. To investigate the nature of the DRG galaxies in our model, we also show the model predictions when no dust extinction is included (Fig. 10, *bottom panel, dashed line*); in such a case, the low-redshift peak disappears, showing that the low-redshift part of the distribution is entirely contributed by heavily extincted galaxies peaking at $z \approx 1$, while at $z \gtrsim 1.5$ the distribution is dominated by galaxies with an old stellar population.

4. SUMMARY AND DISCUSSION

We have included the energy injection from AGN feedback in our semianalytic model of galaxy formation, which self-consistently includes the growth of SMBHs and the corresponding AGN emission. We have focused on the effects of such feedback on the evolution of the galaxy color distribution and found that the inclusion of the energy feedback from AGNs enhances the number of red galaxies at low, intermediate, and high redshifts, to match existing observations up to $z \approx 4$. In particular, we find the following.

1. At low redshifts, the color distribution of bright ($M_r < -22$) galaxies is entirely dominated by red ($u - r > 1.5$) objects (Fig. 2). On the other hand, the color distribution of faint galaxies with ($M_r > -18$) remains peaked at blue ($u - r < 1.5$) colors and is not affected by the AGN feedback.
2. The effect of AGN feedback increases at higher redshifts, enhancing the fraction of red galaxies (Figs. 4, 5, and 6); a bimodal color distribution at $z \gtrsim 1.7$ is only obtained when the AGN feedback is considered (see Fig. 5, *bottom panels*).
3. At $1.5 < z < 2.5$ the model predicts a fraction, 0.31, of EROs (with $R - K > 5$) close to the observed value, 0.35 (see Fig. 8); the predicted surface density at $m_K = 20$ is 6.3×10^3 deg^{-2}, while at $m_K = 22$ it increases to $\approx 3 \times 10^4$ deg^{-2} (Fig. 9).

4. At higher redshift, $2 < z < 4$, the surface density of predicted DRGs (with $J - K > 2.3$) is 1.5×10^3 deg^{-2} at $m_K = 20$, in agreement with observations (Fig. 10), while at $m_K = 22$ the model yields values $\approx 10^4$ deg^{-2}, even slightly larger than current estimates, 6×10^3 deg^{-2}, based on *Hubble Space Telescope* (*HST*) data.

5. The redshift distribution of $m_K < 22$ DRGs is characterized by a major peak at $z \approx 2.5$ and a lower peak at $z \approx 1$ (see Fig. 10); we find that the latter is contributed only by heavily absorbed galaxies, while at $z \gtrsim 1.5$ the distribution is dominated by galaxies with old stellar populations. Such a finding is in agreement with the recent results by Papovich et al. (2006), who measured the same partition in the redshift distribution of DRGs, although in their sample the peak of the lower redshift, extincted galaxies is at the slightly larger $z \approx 1.5$. Our results are also consistent with the observed stronger clustering of high-redshift DRGs compared with their lower redshift counterpart (Grazian et al. 2006).

We stress that in our model the downsizing (i.e., the older ages of stellar population observed in the most massive galaxies) and the appearance of a bimodal color distribution at $z \lesssim 1.5$ are not caused by the effect of AGNs. Indeed, hierarchical models predict that massive objects are assembled from progenitor clumps formed in biased high-density regions of the primordial density field, where the enhanced density allowed early star formation, so they naturally predict older stellar populations to be present in massive galaxies. In our model, the bimodality observed in the galaxy color distribution is the final result of the interplay between the above biasing properties of the primordial density field from which the progenitor of local galaxies have formed, and the dependence of feedback/star formation processes on the depth of the DM potential wells, as we showed in our previous paper (Menci et al. 2005) and also obtained in independent works (Croton et al. 2006, the case with no heating source). Rather, the AGN feedback strongly enhances the proportion of galaxies populating the red (or extremely red) branch of the color distribution, and—in our model—such an enhancement is particularly effective at high z, where the AGN activity is much larger than at present (see Fig. 5, *bottom panels*).

Note that the gas expelled from galaxies by the AGN feedback in our model enriches the hot gas content of the host halo (group or cluster); thus, the AGN feedback is partially counteracted by the cooling of such a hot gas, which may reconvert part of it back to the cold gas at the center of galaxies. The final effect of the AGN feedback depends on the balance of the above two effects.

At high redshifts, the AGN activity is so frequent, and the AGN luminosities so high, that AGN feedback rapidly counteracts such a cooling. The net result is that galaxies retain, on average, a lower amount of cold gas (and hence show redder colors) compared to the case with no AGN feedback (see Fig. 5, *bottom panels*).

At lower redshift, the AGN activity decreases, and the effectiveness of AGN feedback drops. Nevertheless, the effects of the AGN feedback (mainly generated at high redshifts) are not completely erased even at low redshift, since the reconversion of the hot gas in massive halos into the cold phase is suppressed by (1) the lower gas densities in the larger host halos (the radius of groups and clusters has grown), (2) the lower value of the cooling function (which drops for host halo virial temperatures $T > 10^5$ K) halos, and (3) the reheating of cold galactic gas during major mergers, as described in Menci et al. (2005). These processes (also present in our previous papers) allow for the persistence at low z of effects (such as the gas consumption in starbursts by the AGN feedback) mainly active at high redshifts.

Such a latter feature is unique to our model for AGN feedback, directly associated with the impulsive, luminous quasar phase (the main phase of BH growth) triggered by galaxy interactions. During such a phase, a small coupling to the gas is expected for the radiative output; estimates based on the observed wind speeds up to $v_W \approx 0.4c$ suggest values $v_W/2c \approx 10^{-1}$ associated with covering factors of order 10^{-1}, so efficiencies close to our adopted value $f \approx 5 \times 10^{-2}$ are expected. In this phase, gas is swept out of the galactic potential wells in a way similar to that found in the simulation of Di Matteo et al. (2005). Such a mode of AGN feedback differs from that implemented in other recent semianalytic models, in which the outflows are associated (with an efficiency close to 100%) with a lower accretion phase of the AGN, corresponding to accretion rates so low that the AGN is not optically luminous, and which is triggered by gas shock heating (Cattaneo et al. 2006) or by smooth hot gas accretion within a static hot gas halo (Croton et al. 2006; Bower et al. 2005). The feedback associated with such a smooth mode of AGN accretion may start already at $z \approx 3$, but increases with time down to low redshifts. In this respect, the color distribution of galaxies at high redshifts constitutes an important probe to discriminate between the two scenarios of AGN accretion and feedback, pending definite observational evidence for a statistically significant occurrence of strong outflows in massive galaxies.

We thank the referee for helpful comments.

REFERENCES

Baldry, I. K., Glazebrook, K., Brinkmann, J., Zeljko, I., Lupton, R. H., Nichol, R. C., & Szalay, A. S. 2004, ApJ, 600, 681
Begelman, M. C., & Nath, B. B., 2005, MNRAS, 361, 1387
Bell, E., Wolf, C., Meisenheimer, K., Rix, H.-W., Borch, A., Dye, S., Kleineinrich, M., & McIntosh, D. 2004, ApJ, 608, 752
Böringer, H., Voges, W., Fabian, A. C., Edge, A. C., & Neumann, D. M. 1993, MNRAS, 264, L25
Bower, R. G., Benson, A. J., Malbon, R., Helly, J. C., Frenk, C. S., Baugh, C. M., Cole, S., & Lacey, C. G. 2006, MNRAS, in press (astro-ph/0511338)
Boyle, B. J., Shanks, T., Croom, S. M., Smith, R. J., Miller, L., Loaring, N., & Heymans, C. 2000, MNRAS, 317, 1014
Bruzual, A., & Charlot, S. 1993, ApJ, 405, 538
Cattaneo, A., Dekel, A., Devriendt, J., Guiderdoni, B., & Blaizot, J. 2006, MNRAS, submitted (astro-ph/0601295)
Cavaliere, A., Lapi, A., & Menci, N. 2002, ApJ, 581, L1
Cavaliere, A., & Vittorini, V. 2000, ApJ, 543, 599
Chartas, G., Brandt, W. N., & Gallagher, S. C. 2004, in IAU Symp. 222, The Interplay among Black Holes, Stars and ISM in Galactic Nuclei, ed. T. Storchi-Bergmann, L. C. Ho, & H. R. Schmitt (Cambridge: Cambridge Univ. Press), 411
Chartas, G., Brandt, W. N., Gallagher, S. C., & Garmire, G. P. 2002, ApJ, 579, 169
Cimatti, A., et al. 2002, A&A, 381, L68
———. 2004, Nature, 430, 184
Ciotti, L., & Ostriker, J. P. 1997, ApJ, 487, L105
Cole, S., Lacey, C. G., Baugh, C. M., & Frenk, C. S. 2000, MNRAS, 319, 168
Crenshaw, D. M., Kraemer, S. B., & George, I. M. 2003, ARA&A, 41, 117
Croton, D. J., et al. 2006, MNRAS, 365, 11
Daddi, E., Cimatti, A., Pozzetti, L., Hoekstra, H., Rottgering, H., Renzini, A., Zamorani, G., & Mannucci, F. 2000, A&A, 361, 535
Daddi, E., et al. 2005, ApJ, 626, 680
Dahlen, T., et al. 2005, ApJ, 631, 126
Di Matteo, T., Springel, V., & Hernquist, L. 2005, Nature, 433, 604
Elvis, M., et al. 1994, ApJS, 95, 1
Fabian, A. 1999, MNRAS, 308, L39
Fabian, A. C., et al. 2000, MNRAS, 318, L65
Fan, X., et al. 2001, AJ, 121, 54
Ferrarese, L., & Merritt, D. 2000, ApJ, 539, L9
Figuenov, A., Reiprich, T. H., & Böringer, H. 2001, A&A, 368, 749

Fontana, A., et al. 2004, A&A, 424, 23
Franx, M., et al. 2003, ApJ, 587, L79
Gebhardt, K., et al. 2000, ApJ, 539, L13
Giallongo, E., Salimbeni, S., Menci, N., Zamorani, G., Fontana, A., Dickinson, M., Cristiani, S., & Pozzetti, L. 2005, ApJ, 622, 116
Granato, G. L., De Zotti, G., Silva, L., Bressan, A., & Danese, L. 2004, ApJ, 600, 580
Grazian, A., et al. 2006, A&A, 453, 507
Haehnelt, M. J., Natarajan, P., & Rees, M. J. 1998, MNRAS, 300, 817
Hartwick, F. D. A., & Shade, D. 1990, ARA&A, 28, 437
Kang, X., Jing, Y. P., Mo, H. J., & Börner, G. 2005, ApJ, 631, 21
Kang, X., Jing, Y. P., & Silk, J. 2006, ApJ, in press (astro-ph/0601685)
Kauffmann, G., White, S. D. M., & Guiderdoni, B. 1993, MNRAS, 264, 201
Kawata, D., & Gibson, B. K. 2005, MNRAS, 358, L16
Lapi, A., Cavaliere, A., & Menci, N. 2005, ApJ, 619, 60
Lin, Y.-T., Mohr, Y. J., & Stanford, S. A. 2003, ApJ, 591, 749
Madau, P., & Rees, M. J. 2001, ApJ, 551, L27
McCarthy, P. J. 2004, ARA&A, 42, 477
McNamara, B. R., et al. 2000, ApJ, 534, L135
Menci, N., Cavaliere, A., Fontana, A., Giallongo, E., & Poli, F. 2002, ApJ, 575, 18
Menci, N., Cavaliere, A., Fontana, A., Giallongo, E., Poli, F., & Vittorini, V. 2003, ApJ, 587, L63
Menci, N., Fiore, F., Perola, G. C., & Cavaliere, A. 2004, ApJ, 604, 12
Menci, N., Fontana, A., Giallongo, E., & Salimbeni, S. 2005, ApJ, 632, 49
Miyazaki, M., et al. 2003, PASJ, 55, 1079
Mo, H. J., Mao, S., & White, S. D. M. 1998, MNRAS, 295, 319
Monaco, P., & Fontanot, F. 2005, MNRAS, 359, 283
Morganti, R., Tadhunter, C. N., & Oosterloo, T. A. 2005, A&A, 444, L9
Murray, N., Quataert, E., & Thompson, T. A. 2005, ApJ, 618, 569
Okamoto, T., & Nagashima, M. 2003, ApJ, 587, 500
Papovich, C., et al. 2006, ApJ, 640, 92
Pounds, K., King, A. R., Page, K. L., & O'Brien, P. T. 2003, MNRAS, 346, 1025
Roche, N. D., Dunlop, J., & Almaini, O. 2003, MNRAS, 346, 803
Saslaw, W. C. 1985, Gravitational Physics of Stellar and Galactic Systems (Cambridge: Cambridge Univ. Press)
Scannapieco, E., & Oh, S. P. 2004, ApJ, 608, 62
Scannapieco, E., Silk, J., & Bouwens, R. 2005, ApJ, 635, L13
Silk, J., & Rees, M. J. 1998, A&A, 331, L1
Somerville, R. S., & Primack, J. R. 1999, MNRAS, 310, 1087
Somerville, R. S., Primack, J. R., & Faber, S. M. 2001, MNRAS, 320, 504
Somerville, R. S., et al. 2004, ApJ, 600, L135
Strateva, I., et al. 2001, AJ, 122, 1861
van Dokkum, P. G., et al. 2003, ApJ, 587, L83
Yu, Q., & Tremaine, S. 2002, MNRAS, 335, 965